



CERN-EP-2021-151
23 July 2021

Measurement of the groomed jet radius and momentum splitting fraction in pp and Pb–Pb collisions at $\sqrt{s_{\text{NN}}} = 5.02$ TeV

ALICE Collaboration*

Abstract

This article presents groomed jet substructure measurements in pp and Pb–Pb collisions at $\sqrt{s_{\text{NN}}} = 5.02$ TeV with the ALICE detector. The Soft Drop grooming algorithm provides access to the hard parton splittings inside a jet by removing soft wide-angle radiation. We report the groomed jet momentum splitting fraction, z_{g} , and the (scaled) groomed jet radius, θ_{g} . Charged-particle jets are reconstructed at midrapidity using the anti- k_{T} algorithm with resolution parameters $R = 0.2$ and $R = 0.4$. In heavy-ion collisions, the large underlying event poses a challenge for the reconstruction of groomed jet observables, since fluctuations in the background can cause groomed parton splittings to be misidentified. By using strong grooming conditions to reduce this background, we report these observables fully corrected for detector effects and background fluctuations for the first time. A narrowing of the θ_{g} distribution in Pb–Pb collisions compared to pp collisions is seen, which provides direct evidence of the modification of the angular structure of jets in the quark–gluon plasma. No significant modification of the z_{g} distribution in Pb–Pb collisions compared to pp collisions is observed. These results are compared with a variety of theoretical models of jet quenching, and provide constraints on jet energy-loss mechanisms and coherence effects in the quark–gluon plasma.

arXiv:2107.12984v2 [nucl-ex] 7 Apr 2022

*See Appendix A for the list of collaboration members

1 Introduction

Ultrarelativistic heavy-ion collisions at the Large Hadron Collider (LHC) are used to study the high temperature deconfined phase of strongly interacting matter known as the quark–gluon plasma (QGP) [1–5]. Highly-energetic jets created early in the collisions interact with the QGP medium and through those interactions they can lose energy and their internal structure can be modified. This process, known as jet quenching, can be used to reveal the physical properties of the QGP itself such as its transport coefficients and the quasi-particle nature of its degrees of freedom as a function of scale [6–9]. Experimentally, jet quenching is evaluated by comparing jet measurements in heavy-ion collisions to analogous measurements in pp collisions [10–18]. Notably, measurements of the jet angularity [16] and jet transverse profile [18], which are sensitive to a combination of the angular and momentum space structure of jets, suggest a narrowing of the jet core in heavy-ion collisions. Nonetheless, up to now, no direct modification of the intra-jet angular distribution alone has been measured.

Jet grooming algorithms provide access to the hard (high-momentum transfer) parton splittings inside a jet by removing soft wide-angle radiation [19–21]. Access to the hard splittings isolates substructures that are well-controlled in perturbative QCD (pQCD), which in heavy-ion collisions may help constrain various jet quenching effects such as energy loss, transverse-momentum broadening, and color coherence. Measurements of groomed jet observables in heavy-ion collisions have been performed by the ALICE and CMS collaborations [22–24], and opened a new avenue in the study of jet substructure in heavy-ion collisions.

The Soft Drop (SD) [19–21] grooming algorithm identifies a single splitting by first reconstructing a jet with the anti- k_T algorithm and then reclustering the constituents of the jet using the Cambridge/Aachen (C/A) algorithm [25] in order to follow the angular ordering of the QCD parton shower. The splitting is selected from within the history of the reclustering with a grooming condition, $z > z_{\text{cut}}\theta^\beta$, where β and z_{cut} are tunable parameters, z is the fraction of transverse momentum (p_T) carried by the sub-leading (lowest p_T) prong,

$$z \equiv \frac{p_{T,\text{subleading}}}{p_{T,\text{leading}} + p_{T,\text{subleading}}}, \quad (1)$$

and θ is the relative angular distance between the leading and sub-leading prong,

$$\theta \equiv \frac{\sqrt{\Delta y^2 + \Delta\phi^2}}{R}, \quad (2)$$

where Δy and $\Delta\phi$ are the distances measured in rapidity and azimuthal angle, respectively, and R is the jet resolution parameter. The groomed splitting is then characterized by two relevant kinematic observables: the groomed momentum fraction, z_g , and the (scaled) groomed jet radius, θ_g , which are the values of z and θ of Eq. (1) and (2) for the identified splitting, as shown in Fig. 1.

In pp collisions, measurements of the θ_g and z_g distributions were performed at RHIC and the LHC [23, 26–29]. At high-transverse momentum p_T , the data are described within uncertainties by pQCD predictions [30].

In heavy-ion collisions, it was proposed that θ_g may be sensitive to several important jet-quenching physics mechanisms: the relative suppression of gluon vs. quark jets, transverse-momentum broadening, and the ability of the medium to resolve a color dipole as two independent color charges [31, 32]. Uncertainty principle arguments suggest that wider splittings are formed earlier in vacuum than narrower splittings ($t_f \sim 1/\theta_g^2$ where t_f is the splitting formation time). In heavy-ion collisions, this would result in wider splittings traversing a longer path in the medium on average. Complementary to θ_g , it has been argued that z_g may be sensitive to the modification of the DGLAP splitting function in the QGP, the breaking of color-coherence, and the response of the medium to the jet [33–36]. By measuring both θ_g and z_g simultaneously, and thereby both the angular and momentum scales of the hard substructure of jets, these jet quenching mechanisms can be further constrained.

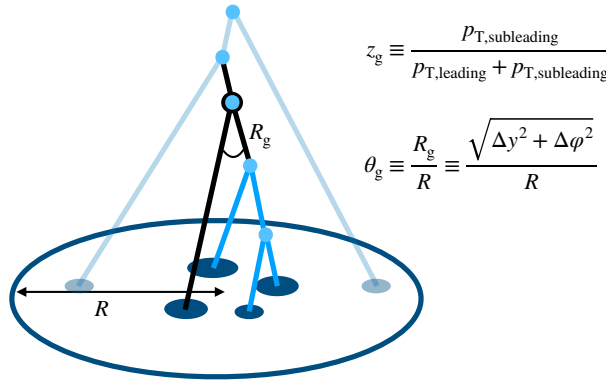


Figure 1: Graphical representation of the angularly ordered Cambridge-Aachen reclustering of jet constituents and subsequent Soft Drop grooming procedure [19], with the identified splitting denoted in black and the splittings that were groomed away in light blue.

Up to now, no measurement of θ_g has been performed in heavy-ion collisions. Previous measurements of the z_g distribution by the CMS [22] and ALICE collaborations [23] indicated significant modification with respect to pp collisions. However, these results were not corrected for background and detector effects, and are difficult to compare directly to theoretical calculations [37]. In this letter, we report the first fully corrected measurement of groomed substructure observables in heavy-ion collisions, allowing for a rigorous comparison with theoretical calculations.

2 Experimental setup and data sets

A description of the ALICE detector and its performance can be found in Refs. [38, 39]. The pp data set used in this analysis was collected in 2017 during LHC Run 2 at $\sqrt{s} = 5.02$ TeV using a minimum-bias (MB) trigger defined by the coincidence of the signals from two scintillator arrays in the forward region (V0 detectors) [40]. The Pb–Pb data set was collected in 2018 at $\sqrt{s_{NN}} = 5.02$ TeV. Central and semi-central triggers that select events in the 0–10% and 30–50% centrality intervals based on the multiplicity of produced particles in the forward V0 detectors, were used [41, 42]. The event selection includes a primary-vertex selection and the removal of beam-induced background events and pileup [10]. After these selections, the pp data sample contains 870 million events and corresponds to an integrated luminosity of $18.0 \pm 0.4 \text{ nb}^{-1}$ [43]. The Pb–Pb data sample contains 92 million events in central collisions and 90 million events in semi-central collisions, corresponding to an integrated luminosity of 0.12 nb^{-1} and 0.06 nb^{-1} , respectively.

This analysis uses charged-particle tracks reconstructed using information from both the Time Projection Chamber (TPC) [44] and the Inner Tracking System (ITS) [45]. While track-based observables are collinear-unsafe [46–48], they can be measured with greater precision than calorimeter-based observables and recent measurements have demonstrated that for the groomed jet observables considered here, track-based distributions are compatible with the corresponding collinear-safe distributions [49]. Tracks with $0.15 < p_T < 100 \text{ GeV}/c$ were accepted over pseudorapidity range $|\eta| < 0.9$. Further details about the track selection are described in Ref. [50]. The accepted tracks exhibit approximately uniform azimuthal acceptance and momentum resolution $\sigma(p_T)/p_T$ ranging from about 1% at track $p_T = 1 \text{ GeV}/c$ to 4% at track $p_T = 50 \text{ GeV}/c$.

3 Analysis method

Jets were reconstructed from charged-particle tracks with FastJet 3.2.1 [51] using the anti- k_T algorithm with E -scheme recombination for resolution parameters $R = 0.2$ and 0.4 [52, 53]. The pion mass is

assumed for all jet constituents. Jets in heavy-ion collisions have a large uncorrelated background contribution due to fluctuations in the underlying event (UE) [54]. The event-by-event constituent subtraction method was used, which corrects the overall jet p_T and its substructure simultaneously by subtracting UE energy constituent by constituent [55, 56]. A maximum recombination distance $R_{\max} = 0.25$ was used. After background subtraction, the measured range is $40 < p_{T, \text{ch jet}} < 120 \text{ GeV}/c$. The jet axis is required to be within the fiducial volume of the TPC, $|\eta_{\text{jet}}| < 0.9 - R$, where η_{jet} is the jet pseudorapidity.

Local background fluctuations in a heavy-ion collision environment can result in an incorrect splitting (unrelated to the hard scattering) being identified by the grooming algorithm. In order to address this issue, the measurement was performed by applying a strong grooming condition, $z_{\text{cut}} = 0.2$ (with $\beta = 0$), which better mitigates these effects as compared to softer grooming conditions (e.g. $z_{\text{cut}} = 0.1$) [37]. To further reduce the mistagging effects, we report measurements with either a small resolution parameter ($R = 0.2$ in central collisions) or with more peripheral collisions (30–50% for $R = 0.4$).

The rate of prong mistagging from residual background effects was evaluated by embedding jets simulated with the PYTHIA8 event generator [57] into measured Pb–Pb data and following the procedure in Ref. [37]. The residual background contribution ranges from approximately 5% up to 15% at lower p_T , in more central events, and at larger R . This level of background contamination is small enough to allow the results to be unfolded for detector effects and background fluctuations. The impact of the residual background contribution remains one of the main sources of systematic uncertainty [50].

The reconstructed $p_{T, \text{ch jet}}$, θ_g , and z_g distributions were corrected for effects related to the tracking inefficiency, particle-material interactions, and track p_T resolution. Moreover, in Pb–Pb collisions, background fluctuations significantly smear the reconstructed distributions of θ_g and z_g . To account for these effects, events were simulated with the PYTHIA8 generator using the Monash 2013 tune [57] and the GEANT3 model [58] for the particle transport in the ALICE detectors' material. For the Pb–Pb data, we embedded the simulated events into measured Pb–Pb data to mimic the background effects. A four-dimensional response matrix describing the detector and background response in $p_{T, \text{ch jet}}$ and θ_g or z_g was constructed and used in the two-dimensional unfolding in $p_{T, \text{ch jet}}$, θ_g or z_g using the iterative Bayesian unfolding algorithm [59, 60].

4 Systematic uncertainties

The largest systematic uncertainties in this measurement originate from the tracking inefficiency, the unfolding procedure, residual mistagged prongs, and the background subtraction procedure. The total systematic uncertainty is calculated as the quadratic sum of all of the individual systematic uncertainties described below.

The systematic uncertainty due to the uncertainty of the tracking efficiency is evaluated using random rejection of additional tracks in jet finding according to the estimated tracking efficiency uncertainty of 4%, based on variations in the track selection criteria and on the ITS-TPC track-matching efficiency uncertainty. The systematic uncertainty arising from the unfolding regularization procedure is evaluated by varying the number of unfolding iterations by ± 2 units, scaling the prior distribution, varying the binning, and varying the lower bound in the detector-level charged-particle jet transverse momentum $p_{T, \text{det}}^{\text{ch jet}}$ range by 5 GeV/ c . The systematic uncertainty due to the model-dependence of the generator used to construct the response matrix is estimated by comparing results obtained with PYTHIA [57], HERWIG [61], and JEWEL [62]. The systematic uncertainty due to the bias introduced by the constituent subtraction procedure is estimated by varying R_{\max} from “under-subtraction” ($R_{\max} = 0.05$) to “over-subtraction” ($R_{\max} = 0.7$), around the nominal value of $R_{\max} = 0.25$. The systematic uncertainty due to a possible residual contamination of mistagged splittings after unfolding is estimated with a closure test. The total relative systematic uncertainty ranges from 3–24% for θ_g and 4–10% for z_g . See Ref. [50] for more details about the systematic uncertainties used in this measurement.

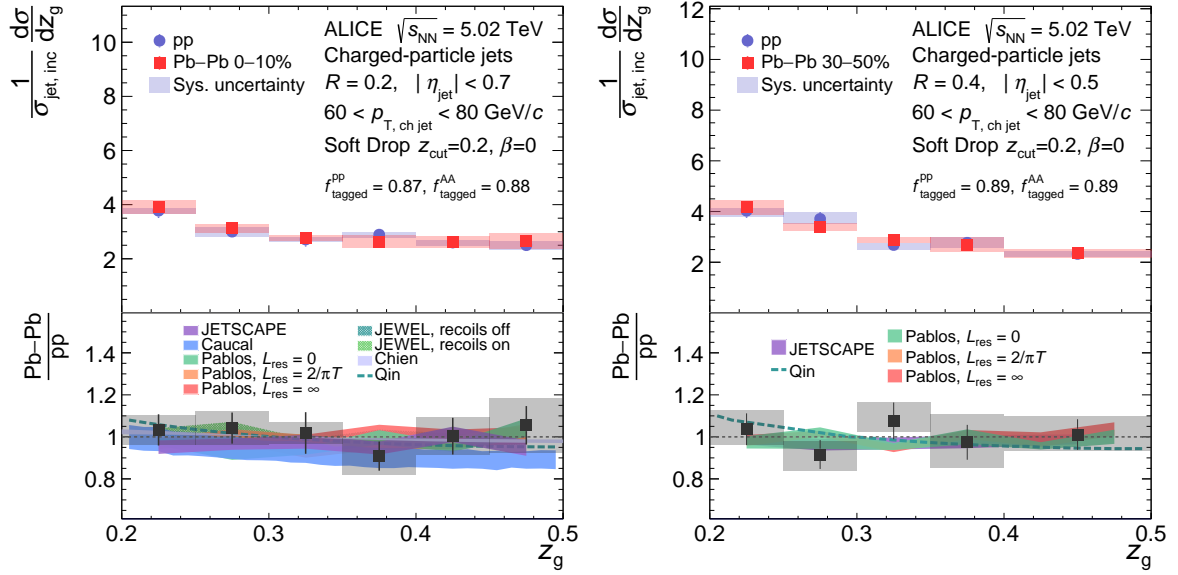


Figure 2: Unfolded z_g distributions for charged-particle jets in pp collisions compared to those in Pb–Pb collisions at $\sqrt{s_{NN}} = 5.02$ TeV with $z_{cut} = 0.2$ for 0–10% centrality for $R = 0.2$ (left) and 30–50% centrality for $R = 0.4$ (right). The distributions are normalized to the inclusive jet cross section in the $60 < p_{T, \text{ch jet}} < 80$ GeV/ c interval, and f_{tagged} indicates the fraction of splittings that were tagged to pass the SD condition in the selected $p_{T, \text{ch jet}}$ interval. The ratios in the bottom panel are compared to the following theoretical predictions: JETSCAPE [63], JEWEL [62, 64], Caucal et al. [34, 65], Chien et al. [33], Qin et al. [35], and Pablos et al. [36, 66, 67]. Further details can be found in Ref. [50].

5 Results

We report the θ_g and z_g distributions in the $p_{T, \text{ch jet}}$ interval between 60 and 80 GeV/ c for $z_{cut} = 0.2$ in central (0–10%, $R = 0.2$) and semi-central (30–50%, $R = 0.4$) Pb–Pb collisions. The distributions are reported as normalized differential cross sections,

$$\frac{1}{\sigma_{\text{jet,inc}}} \frac{d\sigma}{dz_g} = \frac{1}{N_{\text{jet,inc}}} \frac{dN}{dz_g}, \quad (3)$$

where N is the number of jets passing the SD condition with a given $p_{T, \text{ch jet}}$, $N_{\text{jet,inc}}$ is the number of inclusive jets, and $\sigma, \sigma_{\text{jet,inc}}$ are the corresponding cross sections. The analog of Eq. (3) also applies for θ_g .

The z_g and θ_g distributions are shown in Fig. 2 and Fig. 3, respectively. The distributions from Pb–Pb collisions are compared with the corresponding distributions from pp collisions, with their ratios displayed in the bottom panels. The relative uncertainties are assumed to be uncorrelated between pp and Pb–Pb collisions, and are added in quadrature in the ratio. In Pb–Pb collisions the precision of the measurements decreases as the jet resolution parameter is increased or the centrality is decreased, as the prong mistagging probability decreases with centrality and with decreasing R .

The fraction of jets that do not contain a splitting which passes the SD condition (f_{tagged}) differs by at most 1% between Pb–Pb and pp collisions. Therefore, any modifications in Pb–Pb compared to pp collisions can change the shape of the distribution, but keep the integral approximately the same.

The z_g distributions in Pb–Pb and pp collisions are consistent within experimental uncertainties for all jet momenta, jet resolution parameters, and centralities measured.

The situation is remarkably different when comparing the groomed jet radius, θ_g , in both systems. For $R = 0.2$ in central collisions, the data suggests a narrowing of the Pb–Pb distribution relative to the pp

distribution is observed. This narrowing persists even in semi-central Pb–Pb collisions for $R = 0.4$ where quenching effects are expected to be less than in central collisions.

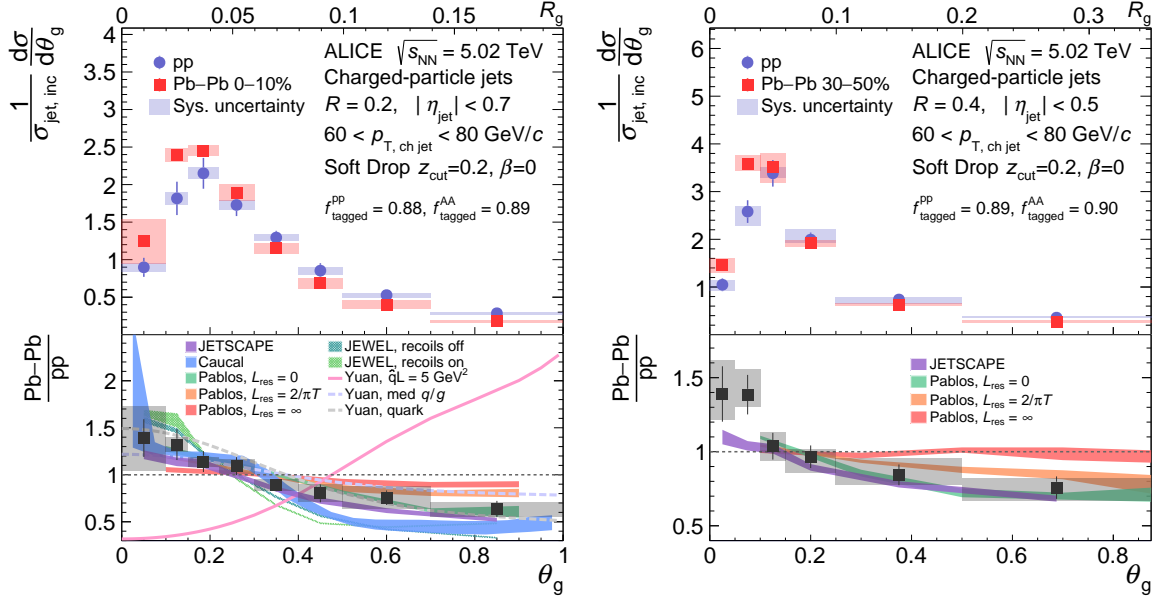


Figure 3: Unfolded θ_g distributions for charged-particle jets in pp collisions compared to those in Pb–Pb collisions at $\sqrt{s_{\text{NN}}} = 5.02$ TeV with $z_{\text{cut}} = 0.2$ for 0–10% centrality for $R = 0.2$ (left) and 30–50% centrality for $R = 0.4$ (right). The distributions are normalized to the inclusive jet cross section in the $60 < p_{\text{T, ch jet}} < 80$ GeV/ c interval, and f_{tagged} indicates the fraction of splittings that were tagged to pass the SD condition in the selected $p_{\text{T, ch jet}}$ interval. The ratios in the bottom panel are compared to the following theoretical predictions: JETSCAPE [63], JEWEL [62, 64], Caucal et al. [34, 65], Pablos et al. [36, 66, 67], and Yuan et al. [31]. Further details can be found in Ref. [50].

We compare the ratio of the measurements in pp and Pb–Pb collisions with several theoretical implementations of jet quenching:

- *JETSCAPE* [63] consists of a medium-modified parton shower with the MATTER model [68] controlling the high-virtuality phase and the Linear Boltzmann Transport (LBT) model describing the low-virtuality phase [69]. The version of JETSCAPE used for this calculation employs a jet transport coefficient, \hat{q} , that includes dependence on parton virtuality, in addition to dependence on the local temperature and running of the parton-medium coupling.
- *JEWEL* [62, 64] consists a Monte Carlo implementation of BDMPS-based medium-induced gluon radiation in a medium modeled with a Bjorken expansion. We consider the impact of medium recoil by including calculations both with and without recoils enabled [70].
- *Caucal et al.* [34, 65] implements a pQCD parton shower with incoherent interactions including both factorized vacuum and medium-induced emissions in a static brick medium.
- *Chien et al.* [33] (for z_g only) applies Soft Collinear Effective Theory with Glauber gluon interactions.
- *Qin et al.* [35] (for z_g only) applies the higher twist formalism with coherent energy loss.
- *Pablos et al.* [36, 66, 67] consists of partons produced by a vacuum shower that interact with the medium according to a strongly-coupled AdS/CFT-based model. The parameter L_{res} describes the degree to which the medium can resolve the jet angular structure, where $L_{\text{res}} = 0$ corresponds to full resolution of all jet constituents (fully incoherent), $L_{\text{res}} = \infty$ corresponds to fully coherent energy loss, and $L_{\text{res}} = 2/\pi T$ is an intermediate case, where T is the local medium temperature.

- *Yuan et al.* [31] (for θ_g only) “med q/g ” and “quark” consist of medium-modified quark-gluon fractions without any additional effects, where the quark-gluon fractions in the “med q/g ” case are extracted in Ref. [71] with a relative suppression factor of approximately four between gluon jets and quark jets. The calculation labeled “ $\hat{q}L$ ” includes an implementation of transverse-momentum broadening.

The Pb–Pb-to-pp ratios of the z_g distributions are consistent with all theoretical predictions considered. The predicted modifications, which have been constrained by previous measurements [22, 23], are small, and the differences between them are yet smaller than the current uncertainty of the data. Nevertheless, these new measurements are the first direct comparisons of predictions to fully corrected data, and limit the possible in-medium modifications of the momentum structure of hard splittings to be less than 10–20% depending on the centrality, jet R , and the grooming settings considered.

Despite employing different microscopic implementations of the jet-medium interactions, the majority of the models capture the qualitative feature of the narrowing seen in the θ_g distributions. The theoretical models can be grouped according to three distinct mechanisms by which θ_g is modified: incoherent energy loss, coherent energy loss, and transverse broadening. The measurements are consistent with models implementing (transverse) incoherent interaction of the jet shower constituents with the medium. This is illustrated by calculations of Pablos et al. where the data favor the incoherent energy loss ($L_{\text{res}} = 0$) and is also supported by Caucal et al., JEWEL, and JETSCAPE. On the other hand, the Yuan et al. calculation with medium-modified “quark–gluon” fractions indicates that the data could be explained by the stronger suppression of gluon showers, which are on average broader, with fully coherent energy loss. These two physics mechanisms — the degree of incoherent energy loss, and the relative quark/gluon suppression — both lead to a suppression of wide-angle splittings. The prediction by Yuan et al. “ $\hat{q}L$ ” exhibits the opposite trend compared to the data, demonstrating that there is no strong transverse broadening in the hard substructure.

The presented measurements indicate that the medium has a significant resolving power for splittings with a particular dependence on the angular (or coherence) scale, promoting narrow structures or filtering out wider jets altogether.

6 Conclusions

We reported the groomed jet momentum fraction, z_g , and the (scaled) groomed jet radius, θ_g , of charged-particle jets measured in pp and Pb–Pb collisions at $\sqrt{s_{\text{NN}}} = 5.02$ TeV with the ALICE detector. By using stronger grooming conditions in the SD grooming algorithm, we suppressed contamination of mistagged splittings from the underlying event, and unfolded the final distributions for detector and background fluctuation effects. This allows for the first time the direct comparison of groomed jet measurements in heavy-ion collisions with theoretical predictions of jet quenching in the QGP. The z_g distributions are consistent with no modification in Pb–Pb collisions compared to pp collisions. The θ_g distributions are narrower in Pb–Pb collisions compared to pp collisions, which is the first direct experimental evidence for the modification of the angular scale of groomed jets in heavy-ion collisions.

These new results demonstrate sensitivity to the microscopic structure of the QGP, including its angular resolving power. This marks an important step towards quantitative understanding of the properties of the QGP, and provides a new path for novel differential jet substructure measurements to further elucidate the microscopic nature of the QGP.

Acknowledgements

We gratefully acknowledge Paul Caucal, Yang-Ting Chien, Daniel Pablos, Chanwook Park, Guang-You Qin, Gregory Soyez, Feng Yuan, and the JETSCAPE Collaboration for providing theoretical predictions. We thank Korinna Zapp for discussions regarding recoil subtraction in the JEWEL model.

The ALICE Collaboration would like to thank all its engineers and technicians for their invaluable contributions to the construction of the experiment and the CERN accelerator teams for the outstanding performance of the LHC complex. The ALICE Collaboration gratefully acknowledges the resources and support provided by all Grid centres and the Worldwide LHC Computing Grid (WLCG) collaboration. The ALICE Collaboration acknowledges the following funding agencies for their support in building and running the ALICE detector: A. I. Alikhanyan National Science Laboratory (Yerevan Physics Institute) Foundation (ANSL), State Committee of Science and World Federation of Scientists (WFS), Armenia; Austrian Academy of Sciences, Austrian Science Fund (FWF): [M 2467-N36] and Nationalstiftung für Forschung, Technologie und Entwicklung, Austria; Ministry of Communications and High Technologies, National Nuclear Research Center, Azerbaijan; Conselho Nacional de Desenvolvimento Científico e Tecnológico (CNPq), Financiadora de Estudos e Projetos (Finep), Fundação de Amparo à Pesquisa do Estado de São Paulo (FAPESP) and Universidade Federal do Rio Grande do Sul (UFRGS), Brazil; Ministry of Education of China (MOEC), Ministry of Science & Technology of China (MSTC) and National Natural Science Foundation of China (NSFC), China; Ministry of Science and Education and Croatian Science Foundation, Croatia; Centro de Aplicaciones Tecnológicas y Desarrollo Nuclear (CEADEN), Cubaenergía, Cuba; Ministry of Education, Youth and Sports of the Czech Republic, Czech Republic; The Danish Council for Independent Research | Natural Sciences, the VILLUM FONDEN and Danish National Research Foundation (DNRF), Denmark; Helsinki Institute of Physics (HIP), Finland; Commissariat à l’Energie Atomique (CEA) and Institut National de Physique Nucléaire et de Physique des Particules (IN2P3) and Centre National de la Recherche Scientifique (CNRS), France; Bundesministerium für Bildung und Forschung (BMBF) and GSI Helmholtzzentrum für Schwerionenforschung GmbH, Germany; General Secretariat for Research and Technology, Ministry of Education, Research and Religions, Greece; National Research, Development and Innovation Office, Hungary; Department of Atomic Energy Government of India (DAE), Department of Science and Technology, Government of India (DST), University Grants Commission, Government of India (UGC) and Council of Scientific and Industrial Research (CSIR), India; Indonesian Institute of Science, Indonesia; Istituto Nazionale di Fisica Nucleare (INFN), Italy; Institute for Innovative Science and Technology, Nagasaki Institute of Applied Science (IIST), Japanese Ministry of Education, Culture, Sports, Science and Technology (MEXT) and Japan Society for the Promotion of Science (JSPS) KAKENHI, Japan; Consejo Nacional de Ciencia (CONACYT) y Tecnología, through Fondo de Cooperación Internacional en Ciencia y Tecnología (FONCICYT) and Dirección General de Asuntos del Personal Académico (DGAPA), Mexico; Nederlandse Organisatie voor Wetenschappelijk Onderzoek (NWO), Netherlands; The Research Council of Norway, Norway; Commission on Science and Technology for Sustainable Development in the South (COMSATS), Pakistan; Pontificia Universidad Católica del Perú, Peru; Ministry of Education and Science, National Science Centre and WUT ID-UB, Poland; Korea Institute of Science and Technology Information and National Research Foundation of Korea (NRF), Republic of Korea; Ministry of Education and Scientific Research, Institute of Atomic Physics and Ministry of Research and Innovation and Institute of Atomic Physics, Romania; Joint Institute for Nuclear Research (JINR), Ministry of Education and Science of the Russian Federation, National Research Centre Kurchatov Institute, Russian Science Foundation and Russian Foundation for Basic Research, Russia; Ministry of Education, Science, Research and Sport of the Slovak Republic, Slovakia; National Research Foundation of South Africa, South Africa; Swedish Research Council (VR) and Knut & Alice Wallenberg Foundation (KAW), Sweden; European Organization for Nuclear Research, Switzerland; Suranaree University of Technology (SUT), National Science and Technology Development Agency (NSDTA) and Office of the Higher Education Commission under NRU project of Thailand, Thailand; Turkish Energy, Nuclear and Mineral

Research Agency (TENMAK), Turkey; National Academy of Sciences of Ukraine, Ukraine; Science and Technology Facilities Council (STFC), United Kingdom; National Science Foundation of the United States of America (NSF) and United States Department of Energy, Office of Nuclear Physics (DOE NP), United States of America.

References

- [1] **STAR** Collaboration, J. Adams *et al.*, “Experimental and theoretical challenges in the search for the quark gluon plasma: The STAR Collaboration’s critical assessment of the evidence from RHIC collisions”, *Nucl. Phys. A* **757** (2005) 102–183, arXiv:nuc1-ex/0501009.
- [2] **PHENIX** Collaboration, K. Adcox *et al.*, “Formation of dense partonic matter in relativistic nucleus-nucleus collisions at RHIC: Experimental evaluation by the PHENIX collaboration”, *Nucl. Phys. A* **757** (2005) 184–283, arXiv:nuc1-ex/0410003.
- [3] B. Müller, J. Schukraft, and B. Wysłouch, “First Results from Pb+Pb Collisions at the LHC”, *Annu. Rev. Nucl. Part. S.* **62** (2012) 361–386.
- [4] P. Braun-Munzinger, V. Koch, T. Schäfer, and J. Stachel, “Properties of hot and dense matter from relativistic heavy ion collisions”, *Phys. Rept.* **621** (2016) 76–126.
- [5] W. Busza, K. Rajagopal, and W. van der Schee, “Heavy Ion Collisions: The Big Picture, and the Big Questions”, *Ann. Rev. Nucl. Part. Sci.* **68** (2018) 339–376.
- [6] J. D. Bjorken, “Highly relativistic nucleus-nucleus collisions: The central rapidity region”, *Phys. Rev. D* **27** (1983) 140–151.
- [7] G.-Y. Qin and X.-N. Wang, “Jet quenching in high-energy heavy-ion collisions”, *Int. J. Mod. Phys. E* **24** (2015) 1530014.
- [8] J.-P. Blaizot and Y. Mehtar-Tani, “Jet structure in heavy ion collisions”, *Int. J. Mod. Phys. E* **24** (2015) 1530012.
- [9] A. Majumder and M. van Leeuwen, “The theory and phenomenology of perturbative QCD based jet quenching”, *Prog. Part. Nucl. Phys.* **66** (2011) 41–92.
- [10] **ALICE** Collaboration, “Measurements of inclusive jet spectra in pp and central Pb–Pb collisions at $\sqrt{s_{NN}} = 5.02$ TeV”, *Phys. Rev. C* **101** (2020) 034911.
- [11] **ATLAS** Collaboration, “Measurement of the nuclear modification factor for inclusive jets in Pb+Pb collisions at $\sqrt{s_{NN}} = 5.02$ TeV with the ATLAS detector”, *Phys. Lett. B* **790** (2019) 108–128.
- [12] **CMS** Collaboration, “Measurement of inclusive jet cross sections in pp and Pb–Pb collisions at $\sqrt{s_{NN}} = 2.76$ TeV”, *Phys. Rev. C* **96** (2017) 015202.
- [13] **STAR** Collaboration, J. Adam *et al.*, “Measurement of inclusive charged-particle jet production in Au + Au collisions at $\sqrt{s_{NN}} = 200$ GeV”, *Phys. Rev. C* **102** no. 5, (2020) 054913, arXiv:2006.00582 [nuc1-ex].
- [14] **ALICE** Collaboration, “Measurement of jet quenching with semi-inclusive hadron-jet distributions in central Pb–Pb collisions at $\sqrt{s_{NN}} = 2.76$ TeV”, *J. High Energ. Phys.* **2015** (2015) 170.
- [15] **STAR** Collaboration, “Measurements of jet quenching with semi-inclusive hadron-jet distributions in Au + Au collisions at $\sqrt{s_{NN}} = 200$ GeV”, *Phys. Rev. C* **96** (2017) 024905.
- [16] **ALICE** Collaboration, “Medium modification of the shape of small-radius jets in central Pb–Pb collisions at $\sqrt{s_{NN}} = 2.76$ TeV”, *J. High Energ. Phys.* **2018** (2018) 139.
- [17] **ATLAS** Collaboration, “Measurement of jet fragmentation in Pb–Pb and pp collisions at $\sqrt{s_{NN}} = 5.02$ TeV with the ATLAS detector”, *Phys. Rev. C* **98** (2018) 024908.
- [18] **CMS** Collaboration, “Modification of jet shapes in Pb–Pb collisions at $\sqrt{s_{NN}} = 2.76$ TeV”, *Physics Letters B* **730** (2014) 243–263.

- [19] A. J. Larkoski, S. Marzani, G. Soyez, and J. Thaler, “Soft Drop”, *J. High Energ. Phys.* **05** (2014) 146.
- [20] M. Dasgupta, A. Fregoso, S. Marzani, and G. P. Salam, “Towards an understanding of jet substructure”, *J. High Energ. Phys.* **09** (2013) 029.
- [21] A. J. Larkoski, S. Marzani, and J. Thaler, “Sudakov Safety in Perturbative QCD”, *Phys. Rev.* **D91** (2015) 111501.
- [22] CMS Collaboration, “Measurement of the Splitting Function in pp and Pb–Pb Collisions at $\sqrt{s_{\text{NN}}} = 5.02$ TeV”, *Phys. Rev. Lett.* **120** (2018) 142302.
- [23] ALICE Collaboration, “Exploration of jet substructure using iterative declustering in pp and Pb–Pb collisions at LHC energies”, *Phys. Lett. B* **802** (2020) 135227.
- [24] CMS Collaboration, “Measurement of the groomed jet mass in Pb–Pb and pp collisions at $\sqrt{s_{\text{NN}}} = 5.02$ TeV”, *J. High Energ. Phys.* **2018** (2018) 161.
- [25] Y. L. Dokshitzer, G. D. Leder, S. Moretti, and B. R. Webber, “Better jet clustering algorithms”, *JHEP* **08** (1997) 001, arXiv:hep-ph/9707323.
- [26] ATLAS Collaboration, “Measurement of soft-drop jet observables in pp collisions with the ATLAS detector at $\sqrt{s_{\text{NN}}} = 13$ TeV”, *Phys. Rev. D* **101** (2020) 052007.
- [27] CMS Collaboration, “Measurement of jet substructure observables in $t\bar{t}$ events from proton-proton collisions at $\sqrt{s} = 13$ TeV”, *Phys. Rev. D* **98** (2018) 092014.
- [28] A. Tripathy, W. Xue, A. Larkoski, S. Marzani, and J. Thaler, “Jet Substructure Studies with CMS Open Data”, *Phys. Rev. D* **96** (2017) 074003.
- [29] STAR Collaboration, J. Adam *et al.*, “Measurement of groomed jet substructure observables in p+p collisions at $\sqrt{s} = 200$ GeV with STAR”, *Phys. Lett. B* **811** (2020) 135846, arXiv:2003.02114 [hep-ex].
- [30] Z.-B. Kang, K. Lee, X. Liu, D. Neill, and F. Ringer, “The soft drop groomed jet radius at NLL”, *J. High Energ. Phys.* **02** (2020) 054, arXiv:1908.01783 [hep-ph].
- [31] F. Ringer, B.-W. Xiao, and F. Yuan, “Can we observe jet P_T -broadening in heavy-ion collisions at the LHC?”, *Phys. Lett. B* **808** (2020) 135634, arXiv:1907.12541 [hep-ph].
- [32] J. Casalderrey-Solana, Y. Mehtar-Tani, C. A. Salgado, and K. Tywoniuk, “New picture of jet quenching dictated by color coherence”, *Phys. Lett. B* **725** (2013) 357–360.
- [33] Y.-T. Chien and I. Vitev, “Probing the Hardest Branching within Jets in Heavy-Ion Collisions”, *Phys. Rev. Lett.* **119** (2017) 112301.
- [34] P. Caucal, E. Iancu, and G. Soyez, “Deciphering the z_g distribution in ultrarelativistic heavy ion collisions”, *J. High Energ. Phys.* **10** (2019) 273.
- [35] N.-B. Chang, S. Cao, and G.-Y. Qin, “Probing medium-induced jet splitting and energy loss in heavy-ion collisions”, *Physics Letters B* **781** (2018) 423–432.
- [36] J. Casalderrey-Solana, G. Milhano, D. Pablos, and K. Rajagopal, “Modification of Jet Substructure in Heavy Ion Collisions as a Probe of the Resolution Length of Quark-Gluon Plasma”, *J. High Energ. Phys.* **01** (2020) 044.
- [37] J. Mulligan and M. Ploskon, “Identifying groomed jet splittings in heavy-ion collisions”, *Phys. Rev. C* **102** (2020) 044913, arXiv:2006.01812 [hep-ph].
- [38] ALICE Collaboration, K. Aamodt *et al.*, “The ALICE experiment at the CERN LHC”, *JINST* **3** (2008) S08002.
- [39] ALICE Collaboration, “Performance of the ALICE Experiment at the CERN LHC”, *Int. J. Mod. Phys. A* **29** (2014) 1430044.
- [40] ALICE Collaboration, “Performance of the ALICE VZERO system”, *JINST* **8** (2013) P10016.
- [41] ALICE Collaboration, “Centrality determination of Pb–Pb collisions at $\sqrt{s_{\text{NN}}} = 2.76$ TeV with ALICE”, *Phys. Rev. C* **88** (2013) 044909.

- [42] ALICE Collaboration, “Centrality determination in heavy-ion collisions.”
<http://cds.cern.ch/record/2636623>.
- [43] ALICE Collaboration, “ALICE 2017 luminosity determination for pp collisions at $\sqrt{s} = 5$ TeV”,
<http://cds.cern.ch/record/2648933>.
- [44] J. Alme and et al., “The ALICE TPC, a large 3-dimensional tracking device with fast readout for ultra-high multiplicity events”, *Nucl. Instrum. Meth. A: Accelerators, Spectrometers, Detectors and Associated Equipment* **622** (2010) 316–367.
- [45] ALICE Collaboration, “Alignment of the ALICE Inner Tracking System with cosmic-ray tracks”, *JINST* **5** (2010) P03003.
- [46] H.-M. Chang, M. Procura, J. Thaler, and W. J. Waalewijn, “Calculating Track-Based Observables for the LHC”, *Phys. Rev. Lett.* **111** (Sep, 2013) 102002, arXiv:1303.6637 [hep-ph].
- [47] H. Chen, I. Moul, X. Zhang, and H. X. Zhu, “Rethinking jets with energy correlators: Tracks, resummation, and analytic continuation”, *Phys. Rev. D* **102** no. 5, (Sep, 2020) 054012, arXiv:2004.11381 [hep-ph].
- [48] Y.-T. Chien, R. Rahn, S. Schrijnder van Velzen, D. Y. Shao, W. J. Waalewijn, and B. Wu, “Recoil-free azimuthal angle for precision boson-jet correlation”, *Phys. Lett. B* **815** (2021) 136124, arXiv:2005.12279 [hep-ph].
- [49] ATLAS Collaboration, G. Aad *et al.*, “Measurement of soft-drop jet observables in pp collisions with the ATLAS detector at $\sqrt{s} = 13$ TeV”, *Phys. Rev. D* **101** no. 5, (2020) 052007, arXiv:1912.09837 [hep-ex].
- [50] ALICE Collaboration, “Supplemental material: Measurements of the groomed jet radius and groomed momentum fraction in pp and Pb–Pb collisions at $\sqrt{s_{NN}} = 5.02$ TeV.”
<https://cds.cern.ch/record/2725572>.
- [51] M. Cacciari, G. P. Salam, and G. Soyez, “FastJet User Manual”, *Eur. Phys. J. C* **72** (2012) 1896.
- [52] M. Cacciari, G. P. Salam, and G. Soyez, “The anti- k_t jet clustering algorithm”, *J. High Energy Phys.* **04** (2008) 063.
- [53] M. Cacciari, G. P. Salam, and G. Soyez, “The Catchment Area of Jets”, *J. High Energy Phys.* **04** (2008) 005.
- [54] ALICE Collaboration, “Measurement of event background fluctuations for charged particle jet reconstruction in Pb–Pb collisions at $\sqrt{s_{NN}} = 2.76$ TeV”, *J. High Energy Phys.* **2012** (2012) 53.
- [55] P. Berta, M. Spousta, D. W. Miller, and R. Leitner, “Particle-level pileup subtraction for jets and jet shapes”, *J. High Energy Phys.* **06** (2014) 092.
- [56] P. Berta, L. Masetti, D. Miller, and M. Spousta, “Pileup and Underlying Event Mitigation with Iterative Constituent Subtraction”, *J. High Energy Phys.* **08** (2019) 175.
- [57] T. Sjostrand, S. Ask, J. R. Christiansen, R. Corke, N. Desai, P. Ilten, S. Mrenna, S. Prestel, C. O. Rasmussen, and P. Z. Skands, “An introduction to PYTHIA 8.2”, *Comput. Phys. Commun.* **191** (2015) 159–177.
- [58] R. Brun, F. Bruyant, M. Maire, A. C. McPherson, and P. Zancarini, *GEANT 3: user’s guide Geant 3.10, Geant 3.11; rev. version*. CERN, Geneva, 1987. <https://cds.cern.ch/record/1119728>.
- [59] G. D’Agostini, “A multidimensional unfolding method based on bayes’ theorem”, *Nucl. Instrum. Meth. A: Accelerators, Spectrometers, Detectors and Associated Equipment* **362** (1995) 487 – 498.
- [60] “RooUnfold.” <http://hepunix.rl.ac.uk/~adye/software/unfold/RooUnfold.html>.
Access date: May 31 2020.
- [61] J. Bellm *et al.*, “Herwig 7.0/Herwig++ 3.0 release note”, *Eur. Phys. J. C* **76** no. 4, (Apr, 2016) 196, arXiv:1512.01178 [hep-ph].
- [62] K. C. Zapp, “JEWEL 2.0.0: directions for use”, *Eur. Phys. J. C* **74** no. 2, (2014) 2762, arXiv:1311.0048 [hep-ph].

- [63] **JETSCAPE** Collaboration, J. Putschke *et al.*, “The JETSCAPE framework”, arXiv:1903.07706 [nucl-th].
- [64] K. C. Zapp, F. Krauss, and U. A. Wiedemann, “A perturbative framework for jet quenching”, *J. High Energ. Phys.* **03** (2013) 080, arXiv:1212.1599 [hep-ph].
- [65] P. Caucal, E. Iancu, A. H. Mueller, and G. Soyez, “Vacuum-like jet fragmentation in a dense QCD medium”, *Phys. Rev. Lett.* **120** (2018) 232001, arXiv:1801.09703 [hep-ph].
- [66] J. Casalderrey-Solana, D. C. Gulhan, J. G. Milhano, D. Pablos, and K. Rajagopal, “A Hybrid Strong/Weak Coupling Approach to Jet Quenching”, *J. High Energ. Phys.* **10** (2014) 019, arXiv:1405.3864 [hep-ph]. [Erratum: *JHEP* **09** (2015), 175].
- [67] Z. Hulcher, D. Pablos, and K. Rajagopal, “Resolution Effects in the Hybrid Strong/Weak Coupling Model”, *J. High Energ. Phys.* **03** (2018) 010, arXiv:1707.05245 [hep-ph].
- [68] A. Majumder, “Incorporating Space-Time Within Medium-Modified Jet Event Generators”, *Phys. Rev. C* **88** (2013) 014909, arXiv:1301.5323 [nucl-th].
- [69] Y. He, T. Luo, X.-N. Wang, and Y. Zhu, “Linear Boltzmann Transport for Jet Propagation in the Quark-Gluon Plasma: Elastic Processes and Medium Recoil”, *Phys. Rev. C* **91** (2015) 054908, arXiv:1503.03313 [nucl-th]. [Erratum: *Phys.Rev.C* **97** (2018), 019902].
- [70] R. Kunnawalkam Elayavalli and K. C. Zapp, “Medium response in JEWEL and its impact on jet shape observables in heavy ion collisions”, *JHEP* **07** (2017) 141, arXiv:1707.01539 [hep-ph].
- [71] J.-W. Qiu, F. Ringer, N. Sato, and P. Zurita, “Factorization of jet cross sections in heavy-ion collisions”, *Phys. Rev. Lett.* **122** (2019) 252301.

A The ALICE Collaboration

S. Acharya¹⁴³, D. Adamová⁹⁸, A. Adler⁷⁶, G. Aglieri Rinella³⁵, M. Agnello³¹, N. Agrawal⁵⁵, Z. Ahammed¹⁴³, S. Ahmad¹⁶, S.U. Ahn⁷⁸, I. Ahuja³⁹, Z. Akbar⁵², A. Akindinov⁹⁵, M. Al-Turany¹¹⁰, S.N. Alam^{16,41}, D. Aleksandrov⁹¹, B. Alessandro⁶¹, H.M. Alfanda⁷, R. Alfaro Molina⁷³, B. Ali¹⁶, Y. Ali¹⁴, A. Alici²⁶, N. Alizadehvandchali¹²⁷, A. Alkin³⁵, J. Alme²¹, T. Alt⁷⁰, L. Altenkamper²¹, I. Altsybeev¹¹⁵, M.N. Anaam⁷, C. Andrei⁴⁹, D. Andreou⁹³, A. Andronic¹⁴⁶, M. Angeletti³⁵, V. Anguelov¹⁰⁷, F. Antinori⁵⁸, P. Antonioli⁵⁵, C. Anuj¹⁶, N. Apadula⁸², L. Aphecetche¹¹⁷, H. Appelshäuser⁷⁰, S. Arcelli²⁶, R. Arnaldi⁶¹, I.C. Arsene²⁰, M. Arslanok^{148,107}, A. Augustinus³⁵, R. Averbeck¹¹⁰, S. Aziz⁸⁰, M.D. Azmi¹⁶, A. Badalà⁵⁷, Y.W. Baek⁴², X. Bai^{131,110}, R. Bailhache⁷⁰, Y. Bailung⁵¹, R. Bala¹⁰⁴, A. Balbino³¹, A. Baldisseri¹⁴⁰, B. Balis², M. Ball⁴⁴, D. Banerjee⁴, R. Barbera²⁷, L. Barioglio¹⁰⁸, M. Barlou⁸⁷, G.G. Barnaföldi¹⁴⁷, L.S. Barnby⁹⁷, V. Barret¹³⁷, C. Bartels¹³⁰, K. Barth³⁵, E. Bartsch⁷⁰, F. Baruffaldi²⁸, N. Bastid¹³⁷, S. Basu⁸³, G. Batigne¹¹⁷, B. Batyunya⁷⁷, D. Bauri⁵⁰, J.L. Bazo Alba¹¹⁴, I.G. Bearden⁹², C. Beattie¹⁴⁸, I. Belikov¹³⁹, A.D.C. Bell Hechavarria¹⁴⁶, F. Bellini²⁶, R. Bellwied¹²⁷, S. Belokurova¹¹⁵, V. Belyaev⁹⁶, G. Bencedi⁷¹, S. Beole²⁵, A. Bercuci⁴⁹, Y. Berdnikov¹⁰¹, A. Berdnikova¹⁰⁷, L. Bergmann¹⁰⁷, M.G. Besoiu⁶⁹, L. Betev³⁵, P.P. Bhaduri¹⁴³, A. Bhasin¹⁰⁴, I.R. Bhat¹⁰⁴, M.A. Bhat⁴, B. Bhattacharjee⁴³, P. Bhattacharya²³, L. Bianchi²⁵, N. Bianchi⁵³, J. Bielčik³⁸, J. Bielčíková⁹⁸, J. Biernat¹²⁰, A. Bilandzic¹⁰⁸, G. Biro¹⁴⁷, S. Biswas⁴, J.T. Blair¹²¹, D. Blau^{91,84}, M.B. Blidaru¹¹⁰, C. Blume⁷⁰, G. Boca^{29,59}, F. Bock⁹⁹, A. Bogdanov⁹⁶, S. Boi²³, J. Bok⁶³, L. Boldizsár¹⁴⁷, A. Bolozdynya⁹⁶, M. Bombara³⁹, P.M. Bond³⁵, G. Bonomi^{142,59}, H. Borel¹⁴⁰, A. Borissov⁸⁴, H. Bossi¹⁴⁸, E. Botta²⁵, L. Bratrud⁷⁰, P. Braun-Munzinger¹¹⁰, M. Bregant¹²³, M. Broz³⁸, G.E. Bruno^{109,34}, M.D. Buckland¹³⁰, D. Budnikov¹¹¹, H. Buesching⁷⁰, S. Bufalino³¹, O. Bugnon¹¹⁷, P. Buhler¹¹⁶, Z. Buthelezi^{74,134}, J.B. Butt¹⁴, S.A. Bysiak¹²⁰, M. Cai^{28,7}, H. Caines¹⁴⁸, A. Caliva¹¹⁰, E. Calvo Villar¹¹⁴, J.M.M. Camacho¹²², R.S. Camacho⁴⁶, P. Camerini²⁴, F.D.M. Canedo¹²³, F. Carnesecchi^{35,26}, R. Caron¹⁴⁰, J. Castillo Castellanos¹⁴⁰, E.A.R. Casula²³, F. Catalano³¹, C. Ceballos Sanchez⁷⁷, P. Chakraborty⁵⁰, S. Chandra¹⁴³, S. Chapeland³⁵, M. Chartier¹³⁰, S. Chattopadhyay¹⁴³, S. Chattopadhyay¹¹², A. Chauvin²³, T.G. Chavez⁴⁶, T. Cheng⁷, C. Cheshkov¹³⁸, B. Cheynis¹³⁸, V. Chibante Barroso³⁵, D.D. Chinellato¹²⁴, S. Cho⁶³, P. Chochula³⁵, P. Christakoglou⁹³, C.H. Christensen⁹², P. Christiansen⁸³, T. Chujo¹³⁶, C. Cicalo⁵⁶, L. Cifarelli²⁶, F. Cindolo⁵⁵, M.R. Ciupek¹¹⁰, G. Claai^{11,55}, J. Cleymans^{1,126}, F. Colamaria⁵⁴, J.S. Colburn¹¹³, D. Colella^{109,54,34,147}, A. Collu⁸², M. Colocci³⁵, M. Concas^{111,61}, G. Conesa Balbastre⁸¹, Z. Conesa del Valle⁸⁰, G. Contin²⁴, J.G. Contreras³⁸, M.L. Coquet¹⁴⁰, T.M. Cormier⁹⁹, P. Cortese³², M.R. Cosentino¹²⁵, F. Costa³⁵, S. Costanza^{29,59}, P. Crochet¹³⁷, R. Cruz-Torres⁸², E. Cuautle⁷¹, P. Cui⁷, L. Cunqueiro⁹⁹, A. Dainese⁵⁸, M.C. Danisch¹⁰⁷, A. Danu⁶⁹, I. Das¹¹², P. Das⁸⁹, P. Das⁴, S. Das⁴, S. Dash⁵⁰, S. De⁸⁹, A. De Caro³⁰, G. de Cataldo⁵⁴, L. De Cilladi²⁵, J. de Cuveland⁴⁰, A. De Falco²³, D. De Gruttola³⁰, N. De Marco⁶¹, C. De Martin²⁴, S. De Pasquale³⁰, S. Deb⁵¹, H.F. Degenhardt¹²³, K.R. Deja¹⁴⁴, L. Dello Stritto³⁰, S. Delsanto²⁵, W. Deng⁷, P. Dhankher¹⁹, D. Di Bari³⁴, A. Di Mauro³⁵, R.A. Diaz⁸, T. Dietel¹²⁶, Y. Ding^{138,7}, R. Divià³⁵, D.U. Dixit¹⁹, Ø. Djuvsland²¹, U. Dmitrieva⁶⁵, J. Do⁶³, A. Dobrin⁶⁹, B. Dönigus⁷⁰, O. Dordic²⁰, A.K. Dubey¹⁴³, A. Dubla^{110,93}, S. Dudi¹⁰³, M. Dukhishyam⁸⁹, P. Dupieux¹³⁷, N. Dzalaiova¹³, T.M. Eder¹⁴⁶, R.J. Ehlers⁹⁹, V.N. Eikeland²¹, F. Eisenhut⁷⁰, D. Elia⁵⁴, B. Erasmus¹¹⁷, F. Ercolessi²⁶, F. Erhardt¹⁰², A. Erokhin¹¹⁵, M.R. Ersdal²¹, B. Espagnon⁸⁰, G. Eulisse³⁵, D. Evans¹¹³, S. Evdokimov⁹⁴, L. Fabbietti¹⁰⁸, M. Faggin²⁸, J. Faivre⁸¹, F. Fan⁷, A. Fantoni⁵³, M. Fasel⁹⁹, P. Fedichio³¹, A. Feliciello⁶¹, G. Feofilov¹¹⁵, A. Fernández Téllez⁴⁶, A. Ferrero¹⁴⁰, A. Ferretti²⁵, V.J.G. Feuillard¹⁰⁷, J. Figiel¹²⁰, S. Filchagin¹¹¹, D. Finogeev⁶⁵, F.M. Fionda^{56,21}, G. Fiorenza^{35,109}, F. Flor¹²⁷, A.N. Flores¹²¹, S. Foertsch⁷⁴, P. Foka¹¹⁰, S. Fokin⁹¹, E. Fragiaco⁶², E. Frajna¹⁴⁷, U. Fuchs³⁵, N. Funicello³⁰, C. Furget⁸¹, A. Furs⁶⁵, J.J. Gaardhøje⁹², M. Gagliardi²⁵, A.M. Gago¹¹⁴, A. Gal¹³⁹, C.D. Galvan¹²², P. Ganoti⁸⁷, C. Garabatos¹¹⁰, J.R.A. Garcia⁴⁶, E. Garcia-Solis¹⁰, K. Garg¹¹⁷, C. Gargiulo³⁵, A. Garibli⁹⁰, K. Garner¹⁴⁶, P. Gasik¹¹⁰, E.F. Gauger¹²¹, A. Gautam¹²⁹, M.B. Gay Ducati⁷², M. Germain¹¹⁷, P. Ghosh¹⁴³, S.K. Ghosh⁴, M. Giacalone²⁶, P. Gianotti⁵³, P. Giubellino^{110,61}, P. Giubilato²⁸, A.M.C. Glaenger¹⁴⁰, P. Glässel¹⁰⁷, D.J.Q. Goh⁸⁵, V. Gonzalez¹⁴⁵, L.H. González-Trueba⁷³, S. Gorbunov⁴⁰, M. Gorgon², L. Görlich¹²⁰, S. Gotovac³⁶, V. Grabski⁷³, L.K. Graczykowski¹⁴⁴, L. Greiner⁸², A. Grelli⁶⁴, C. Grigoras³⁵, V. Grigoriev⁹⁶, S. Grigoryan^{77,1}, O.S. Groettvik²¹, F. Grosa^{35,61}, J.F. Grosse-Oetringhaus³⁵, R. Grosso¹¹⁰, G.G. Guardiano¹²⁴, R. Guernane⁸¹, M. Guilbaud¹¹⁷, K. Gulbrandsen⁹², T. Gunji¹³⁵, W. Guo⁷, A. Gupta¹⁰⁴, R. Gupta¹⁰⁴, S.P. Guzman⁴⁶, L. Gyulai¹⁴⁷, M.K. Habib¹¹⁰, C. Hadjidakis⁸⁰, G. Halimoglu⁷⁰, H. Hamagaki⁸⁵, G. Hamar¹⁴⁷, M. Hamid⁷, R. Hannigan¹²¹, M.R. Haque^{144,89}, A. Harlanderova¹¹⁰, J.W. Harris¹⁴⁸, A. Harton¹⁰, J.A. Hasenbichler³⁵, H. Hassan⁹⁹, D. Hatzifotiadou⁵⁵, P. Hauer⁴⁴, L.B. Havener¹⁴⁸, S. Hayashi¹³⁵, S.T. Heckel¹⁰⁸, E. Hellbär¹¹⁰, H. Helstrup³⁷, T. Herman³⁸, E.G. Hernandez⁴⁶, G. Herrera Corral⁹, F. Herrmann¹⁴⁶, K.F. Hetland³⁷, H. Hillemanns³⁵, C. Hills¹³⁰, B. Hippolyte¹³⁹, B. Hofman⁶⁴, B. Hohlweger⁹³, J. Honeremann¹⁴⁶, G.H. Hong¹⁴⁹, D. Horak³⁸, S. Hornung¹¹⁰, A. Horzyk², R. Hosokawa¹⁵, Y. Hou⁷, P. Hristov³⁵, C. Hughes¹³³, P. Huhn⁷⁰, T.J. Humanic¹⁰⁰, H. Hushnud¹¹², L.A. Husova¹⁴⁶, A. Hutson¹²⁷, D. Hutter⁴⁰, J.P. Iddon^{35,130}, R. Ilkaev¹¹¹, H. Ilyas¹⁴, M. Inaba¹³⁶,

G.M. Innocenti³⁵, M. Ippolitov⁹¹, A. Isakov^{38,98}, M.S. Islam¹¹², M. Ivanov¹¹⁰, V. Ivanov¹⁰¹, V. Izucheev⁹⁴, M. Jablonski², B. Jacak⁸², N. Jacazio³⁵, P.M. Jacobs⁸², S. Jadlovská¹¹⁹, J. Jadlovsky¹¹⁹, S. Jaelani⁶⁴, C. Jahnke^{124,123}, M.J. Jakubowska¹⁴⁴, A. Jalotra¹⁰⁴, M.A. Janik¹⁴⁴, T. Janson⁷⁶, M. Jercic¹⁰², O. Jevons¹¹³, A.A.P. Jimenez⁷¹, F. Jonas^{99,146}, P.G. Jones¹¹³, J.M. Jowett^{35,110}, J. Jung⁷⁰, M. Jung⁷⁰, A. Junique³⁵, A. Jusko¹¹³, J. Kaewjai¹¹⁸, P. Kalinak⁶⁶, A. Kalweit³⁵, V. Kaplin⁹⁶, S. Kar⁷, A. Karasu Uysal⁷⁹, D. Karatovic¹⁰², O. Karavichev⁶⁵, T. Karavicheva⁶⁵, P. Karczmarczyk¹⁴⁴, E. Karpechev⁶⁵, A. Kazantsev⁹¹, U. Kebschull⁷⁶, R. Keidel⁴⁸, D.L.D. Keijdener⁶⁴, M. Keil³⁵, B. Ketzer⁴⁴, Z. Khabanova⁹³, A.M. Khan⁷, S. Khan¹⁶, A. Khanzadeev¹⁰¹, Y. Kharlov^{94,84}, A. Khatun¹⁶, A. Khuntia¹²⁰, B. Kileng³⁷, B. Kim^{17,63}, C. Kim¹⁷, D.J. Kim¹²⁸, E.J. Kim⁷⁵, J. Kim¹⁴⁹, J.S. Kim⁴², J. Kim¹⁰⁷, J. Kim¹⁴⁹, J. Kim⁷⁵, M. Kim¹⁰⁷, S. Kim¹⁸, T. Kim¹⁴⁹, S. Kirsch⁷⁰, I. Kisel⁴⁰, S. Kiselev⁹⁵, A. Kisiel¹⁴⁴, J.P. Kitowski², J.L. Klay⁶, J. Klein³⁵, S. Klein⁸², C. Klein-Bösing¹⁴⁶, M. Kleiner⁷⁰, T. Klemenz¹⁰⁸, A. Kluge³⁵, A.G. Knospe¹²⁷, C. Kobdaj¹¹⁸, M.K. Köhler¹⁰⁷, T. Kollegger¹¹⁰, A. Kondratyev⁷⁷, N. Kondratyeva⁹⁶, E. Kondratyuk⁹⁴, J. König⁷⁰, S.A. Königstorfer¹⁰⁸, P.J. Konopka^{35,2}, G. Kornakov¹⁴⁴, S.D. Koryciak², L. Koska¹¹⁹, A. Kotliarov⁹⁸, O. Kovalenko⁸⁸, V. Kovalenko¹¹⁵, M. Kowalski¹²⁰, I. Králik⁶⁶, A. Kravčáková³⁹, L. Kreis¹¹⁰, M. Krivda^{113,66}, F. Krizek⁹⁸, K. Krizkova Gajdosova³⁸, M. Kroesen¹⁰⁷, M. Krüger⁷⁰, E. Kryshen¹⁰¹, M. Krzewicki⁴⁰, V. Kučera³⁵, C. Kuhn¹³⁹, P.G. Kuijter⁹³, T. Kumaoka¹³⁶, D. Kumar¹⁴³, L. Kumar¹⁰³, N. Kumar¹⁰³, S. Kundu^{35,89}, P. Kurashvili⁸⁸, A. Kurepin⁶⁵, A.B. Kurepin⁶⁵, A. Kuryakin¹¹¹, S. Kuschpil⁹⁸, J. Kvapil¹¹³, M.J. Kweon⁶³, J.Y. Kwon⁶³, Y. Kwon¹⁴⁹, S.L. La Pointe⁴⁰, P. La Rocca²⁷, Y.S. Lai⁸², A. Lakrathok¹¹⁸, M. Lamanna³⁵, R. Langoy¹³², K. Lapidus³⁵, P. Larionov^{35,53}, E. Laudi³⁵, L. Lautner^{35,108}, R. Lavicka³⁸, T. Lazareva¹¹⁵, R. Lea^{142,24,59}, J. Lehrbach⁴⁰, R.C. Lemmon⁹⁷, I. León Monzón¹²², E.D. Lesser¹⁹, M. Lettrich^{35,108}, P. Lévai¹⁴⁷, X. Li¹¹, X.L. Li⁷, J. Lien¹³², R. Lietava¹¹³, B. Lim¹⁷, S.H. Lim¹⁷, V. Lindenstruth⁴⁰, A. Lindner⁴⁹, C. Lippmann¹¹⁰, A. Liu¹⁹, D.H. Liu⁷, J. Liu¹³⁰, I.M. Lofnes²¹, V. Loginov⁹⁶, C. Loizides⁹⁹, P. Loncar³⁶, J.A. Lopez¹⁰⁷, X. Lopez¹³⁷, E. López Torres⁸, J.R. Luhder¹⁴⁶, M. Lunardon²⁸, G. Luparello⁶², Y.G. Ma⁴¹, A. Maevskaya⁶⁵, M. Mager³⁵, T. Mahmoud⁴⁴, A. Maire¹³⁹, M. Malaev¹⁰¹, N.M. Malik¹⁰⁴, Q.W. Malik²⁰, L. Malinina^{IV,77}, D. Mal'Kevich⁹⁵, N. Mallick⁵¹, P. Malzacher¹¹⁰, G. Mandaglio^{33,57}, V. Manko⁹¹, F. Manso¹³⁷, V. Manzari⁵⁴, Y. Mao⁷, J. Mares⁶⁸, G.V. Margagliotti²⁴, A. Margotti⁵⁵, A. Marín¹¹⁰, C. Markert¹²¹, M. Marquard⁷⁰, N.A. Martin¹⁰⁷, P. Martinengo³⁵, J.L. Martinez¹²⁷, M.I. Martínez⁴⁶, G. Martínez García¹¹⁷, S. Masciocchi¹¹⁰, M. Masera²⁵, A. Masoni⁵⁶, L. Massacrier⁸⁰, A. Mastroserio^{141,54}, A.M. Mathis¹⁰⁸, O. Matonoha⁸³, P.F.T. Matuoka¹²³, A. Matyja¹²⁰, C. Mayer¹²⁰, A.L. Mazuecos³⁵, F. Mazzaschi²⁵, M. Mazzilli³⁵, M.A. Mazzoni^{I,60}, J.E. Mdhuli¹³⁴, A.F. Mechler⁷⁰, F. Meddi²², Y. Melikyan⁶⁵, A. Menchaca-Rocha⁷³, E. Meninno^{116,30}, A.S. Menon¹²⁷, M. Meres¹³, S. Mhlanga^{126,74}, Y. Miake¹³⁶, L. Micheletti^{61,25}, L.C. Migliorin¹³⁸, D.L. Mihaylov¹⁰⁸, K. Mikhaylov^{77,95}, A.N. Mishra¹⁴⁷, D. Miśkowiec¹¹⁰, A. Modak⁴, A.P. Mohanty⁶⁴, B. Mohanty⁸⁹, M. Mohisin Khan^{V,16}, M.A. Molander⁴⁵, Z. Moravcova⁹², C. Mordasini¹⁰⁸, D.A. Moreira De Godoy¹⁴⁶, L.A.P. Moreno⁴⁶, I. Morozov⁶⁵, A. Morsch³⁵, T. Mrnjavac³⁵, V. Muccifora⁵³, E. Mudnic³⁶, D. Mühlheim¹⁴⁶, S. Muhuri¹⁴³, J.D. Mulligan⁸², A. Mulliri²³, M.G. Munhoz¹²³, R.H. Munzer⁷⁰, H. Murakami¹³⁵, S. Murray¹²⁶, L. Musa³⁵, J. Musinsky⁶⁶, J.W. Myrcha¹⁴⁴, B. Naik^{134,50}, R. Nair⁸⁸, B.K. Nandi⁵⁰, R. Nania⁵⁵, E. Nappi⁵⁴, A.F. Nassirpour⁸³, A. Nath¹⁰⁷, C. Natrass¹³³, A. Neagu²⁰, L. Nellen⁷¹, S.V. Nesbo³⁷, G. Neskovic⁴⁰, D. Nesterov¹¹⁵, B.S. Nielsen⁹², S. Nikolaev⁹¹, S. Nikulin⁹¹, V. Nikulin¹⁰¹, F. Noferini⁵⁵, S. Noh¹², P. Nomokonov⁷⁷, J. Norman¹³⁰, N. Novitzky¹³⁶, P. Nowakowski¹⁴⁴, A. Nyanin⁹¹, J. Nystrand²¹, M. Ogino⁸⁵, A. Ohlson⁸³, V.A. Okorokov⁹⁶, J. Oliencz¹⁴⁴, A.C. Oliveira Da Silva¹³³, M.H. Oliver¹⁴⁸, A. Onnerstad¹²⁸, C. Oppedisano⁶¹, A. Ortiz Velasquez⁷¹, T. Osako⁴⁷, A. Oskarsson⁸³, J. Otwinowski¹²⁰, M. Oya⁴⁷, K. Oyama⁸⁵, Y. Pachmayer¹⁰⁷, S. Padhan⁵⁰, D. Pagano^{142,59}, G. Paic⁷¹, A. Palasciano⁵⁴, J. Pan¹⁴⁵, S. Panebianco¹⁴⁰, P. Pareek¹⁴³, J. Park⁶³, J.E. Parkkila¹²⁸, S.P. Pathak¹²⁷, R.N. Patra^{104,35}, B. Paul²³, H. Pei⁷, T. Peitzmann⁶⁴, X. Peng⁷, L.G. Pereira⁷², H. Pereira Da Costa¹⁴⁰, D. Peresunko^{91,84}, G.M. Perez⁸, S. Perrin¹⁴⁰, Y. Pestov⁵, V. Petráček³⁸, M. Petrovici⁴⁹, R.P. Pezzi^{117,72}, S. Piano⁶², M. Pikna¹³, P. Pillot¹¹⁷, O. Pinazza^{55,35}, L. Pinsky¹²⁷, C. Pinto²⁷, S. Pisano⁵³, M. Płoskoń⁸², M. Planinic¹⁰², F. Pliquett⁷⁰, M.G. Poghosyan⁹⁹, B. Polichtchouk⁹⁴, S. Politano³¹, N. Poljak¹⁰², A. Pop⁴⁹, S. Porteboeuf-Houssais¹³⁷, J. Porter⁸², V. Pozdniakov⁷⁷, S.K. Prasad⁴, R. Preghenella⁵⁵, F. Prino⁶¹, C.A. Pruneau¹⁴⁵, I. Pshenichnov⁶⁵, M. Puccio³⁵, S. Qiu⁹³, L. Quaglia²⁵, R.E. Quishpe¹²⁷, S. Ragoni¹¹³, A. Rakotozafindrabe¹⁴⁰, L. Ramello³², F. Rami¹³⁹, S.A.R. Ramirez⁴⁶, A.G.T. Ramos³⁴, T.A. Rancien⁸¹, R. Raniwala¹⁰⁵, S. Raniwala¹⁰⁵, S.S. Räsänen⁴⁵, R. Rath⁵¹, I. Ravasenga⁹³, K.F. Read^{99,133}, A.R. Redelbach⁴⁰, K. Redlich^{VI,88}, A. Rehman²¹, P. Reichelt⁷⁰, F. Reidt³⁵, H.A. Reme-ness³⁷, R. Renfordt⁷⁰, Z. Rescakova³⁹, K. Reygers¹⁰⁷, A. Riabov¹⁰¹, V. Riabov¹⁰¹, T. Richert⁸³, M. Richter²⁰, W. Riegler³⁵, F. Riggi²⁷, C. Ristea⁶⁹, M. Rodríguez Cahuantzi⁴⁶, K. Røed²⁰, R. Rogalev⁹⁴, E. Rogochaya⁷⁷, T.S. Rogoschinski⁷⁰, D. Rohr³⁵, D. Röhrich²¹, P.F. Rojas⁴⁶, P.S. Rokita¹⁴⁴, F. Ronchetti⁵³, A. Rosano^{33,57}, E.D. Rosas⁷¹, A. Rossi⁵⁸, A. Rotondi^{29,59}, A. Roy⁵¹, P. Roy¹¹², S. Roy⁵⁰, N. Rubini²⁶, O.V. Rueda⁸³, R. Rui²⁴, B. Ruyantsev⁷⁷, P.G. Russek², A. Rustamov⁹⁰, E. Ryabinkin⁹¹, Y. Ryabov¹⁰¹, A. Rybicki¹²⁰, H. Ryttonen¹²⁸, W. Rzesza¹⁴⁴,

O.A.M. Saarimaki⁴⁵, R. Sadek¹¹⁷, S. Sadovsky⁹⁴, J. Saetre²¹, K. Šafařík³⁸, S.K. Saha¹⁴³, S. Saha⁸⁹, B. Sahoo⁵⁰, P. Sahoo⁵⁰, R. Sahoo⁵¹, S. Sahoo⁶⁷, D. Sahu⁵¹, P.K. Sahu⁶⁷, J. Saini¹⁴³, S. Sakai¹³⁶, S. Sambyal¹⁰⁴, V. Samsonov^{1,101,96}, D. Sarkar¹⁴⁵, N. Sarkar¹⁴³, P. Sarma⁴³, V.M. Sarti¹⁰⁸, M.H.P. Sas¹⁴⁸, J. Schambach^{99,121}, H.S. Scheid⁷⁰, C. Schiaua⁴⁹, R. Schicker¹⁰⁷, A. Schmah¹⁰⁷, C. Schmidt¹¹⁰, H.R. Schmidt¹⁰⁶, M.O. Schmidt³⁵, M. Schmidt¹⁰⁶, N.V. Schmidt^{99,70}, A.R. Schmier¹³³, R. Schotter¹³⁹, J. Schukraft³⁵, Y. Schutz¹³⁹, K. Schwarz¹¹⁰, K. Schweda¹¹⁰, G. Scioli²⁶, E. Scomparin⁶¹, J.E. Seger¹⁵, Y. Sekiguchi¹³⁵, D. Sekihata¹³⁵, I. Selyuzhenkov^{110,96}, S. Senyukov¹³⁹, J.J. Seo⁶³, D. Serebryakov⁶⁵, L. Šerkšnyte¹⁰⁸, A. Sevcenco⁶⁹, T.J. Shaba⁷⁴, A. Shabanov⁶⁵, A. Shabetai¹¹⁷, R. Shahoyan³⁵, W. Shaikh¹¹², A. Shangaraev⁹⁴, A. Sharma¹⁰³, H. Sharma¹²⁰, M. Sharma¹⁰⁴, N. Sharma¹⁰³, S. Sharma¹⁰⁴, U. Sharma¹⁰⁴, O. Sheibani¹²⁷, K. Shigaki⁴⁷, M. Shimomura⁸⁶, S. Shirinkin⁹⁵, Q. Shou⁴¹, Y. Sibiriak⁹¹, S. Siddhanta⁵⁶, T. Siemiarczuk⁸⁸, T.F. Silva¹²³, D. Silvermyr⁸³, G. Simonetti³⁵, B. Singh¹⁰⁸, R. Singh⁸⁹, R. Singh¹⁰⁴, R. Singh⁵¹, V.K. Singh¹⁴³, V. Singhal¹⁴³, T. Sinha¹¹², B. Sitar¹³, M. Sitta³², T.B. Skaali²⁰, G. Skorodumovs¹⁰⁷, M. Slupecki⁴⁵, N. Smirnov¹⁴⁸, R.J.M. Snellings⁶⁴, C. Soncco¹¹⁴, J. Song¹²⁷, A. Songmoolnak¹¹⁸, F. Soramel²⁸, S. Sorensen¹³³, I. Sputowska¹²⁰, J. Stachel¹⁰⁷, I. Stan⁶⁹, P.J. Steffanic¹³³, S.F. Stiefelmaier¹⁰⁷, D. Stocco¹¹⁷, I. Storehaug²⁰, M.M. Storetvedt³⁷, C.P. Stylianidis⁹³, A.A.P. Suaide¹²³, T. Sugitate⁴⁷, C. Suire⁸⁰, M. Sukhanov⁶⁵, M. Suljic³⁵, R. Sultanov⁹⁵, M. Šumbera⁹⁸, V. Sumberia¹⁰⁴, S. Sumowidagdo⁵², S. Swain⁶⁷, A. Szabo¹³, I. Szarka¹³, U. Tabassam¹⁴, S.F. Taghavi¹⁰⁸, G. Taillepiet¹³⁷, J. Takahashi¹²⁴, G.J. Tambave²¹, S. Tang^{137,7}, Z. Tang¹³¹, J.D. Tapia Takaki^{VII,129}, M. Tarhini¹¹⁷, M.G. Tarczila⁴⁹, A. Tauro³⁵, G. Tejada Muñoz⁴⁶, A. Telesca³⁵, L. Terlizzi²⁵, C. Terrevoli¹²⁷, G. Tersimonov³, S. Thakur¹⁴³, D. Thomas¹²¹, R. Tieulent¹³⁸, A. Tikhonov⁶⁵, A.R. Timmins¹²⁷, M. Tkacik¹¹⁹, A. Toia⁷⁰, N. Topilskaya⁶⁵, M. Toppi⁵³, F. Torales-Acosta¹⁹, T. Tork⁸⁰, S.R. Torres³⁸, A. Trifiro^{33,57}, S. Tripathy^{55,71}, T. Tripathy⁵⁰, S. Trogolo^{35,28}, G. Trombetta³⁴, V. Trubnikov³, W.H. Trzaska¹²⁸, T.P. Trzcinski¹⁴⁴, B.A. Trzeciak³⁸, A. Tumkin¹¹¹, R. Turrisi⁵⁸, T.S. Tveter²⁰, K. Ullaland²¹, A. Uras¹³⁸, M. Urioni^{59,142}, G.L. Usai²³, M. Vala³⁹, N. Valle^{59,29}, S. Vallero⁶¹, N. van der Kolk⁶⁴, L.V.R. van Doremalen⁶⁴, M. van Leeuwen⁹³, P. Vande Vyvre³⁵, D. Varga¹⁴⁷, Z. Varga¹⁴⁷, M. Varga-Kofarago¹⁴⁷, A. Vargas⁴⁶, M. Vasileiou⁸⁷, A. Vasiliev⁹¹, O. Vázquez Doce^{53,108}, V. Vechernin¹¹⁵, E. Vercellin²⁵, S. Vergara Limón⁴⁶, L. Vermunt⁶⁴, R. Vértesi¹⁴⁷, M. Verweij⁶⁴, L. Vickovic³⁶, Z. Vilakazi¹³⁴, O. Villalobos Baillie¹¹³, G. Vino⁵⁴, A. Vinogradov⁹¹, T. Virgili³⁰, V. Vislavicius⁹², A. Vodopyanov⁷⁷, B. Volkel³⁵, M.A. Völkl¹⁰⁷, K. Voloshin⁹⁵, S.A. Voloshin¹⁴⁵, G. Volpe³⁴, B. von Haller³⁵, I. Vorobyev¹⁰⁸, D. Voscek¹¹⁹, N. Vozniuk⁶⁵, J. Vrláková³⁹, B. Wagner²¹, C. Wang⁴¹, D. Wang⁴¹, M. Weber¹¹⁶, R.J.G.V. Weelden⁹³, A. Wegrzynek³⁵, S.C. Wenzel³⁵, J.P. Wessels¹⁴⁶, J. Wiechula⁷⁰, J. Wikne²⁰, G. Wilk⁸⁸, J. Wilkinson¹¹⁰, G.A. Willems¹⁴⁶, B. Windelband¹⁰⁷, M. Winn¹⁴⁰, W.E. Witt¹³³, J.R. Wright¹²¹, W. Wu⁴¹, Y. Wu¹³¹, R. Xu⁷, A.K. Yadav¹⁴³, S. Yalcin⁷⁹, Y. Yamaguchi⁴⁷, K. Yamakawa⁴⁷, S. Yang²¹, S. Yano⁴⁷, Z. Yin⁷, H. Yokoyama⁶⁴, I.-K. Yoo¹⁷, J.H. Yoon⁶³, S. Yuan²¹, A. Yuncu¹⁰⁷, V. Zaccolo²⁴, C. Zampolli³⁵, H.J.C. Zanolli⁶⁴, N. Zardoshti³⁵, A. Zarochentsev¹¹⁵, P. Závada⁶⁸, N. Zaviyalov¹¹¹, M. Zhalov¹⁰¹, B. Zhang⁷, S. Zhang⁴¹, X. Zhang⁷, Y. Zhang¹³¹, V. Zhrebchevskii¹¹⁵, Y. Zhi¹¹, N. Zhigareva⁹⁵, D. Zhou⁷, Y. Zhou⁹², J. Zhu^{7,110}, Y. Zhu⁷, A. Zichichi²⁶, G. Zinovjev³, N. Zurlo^{142,59}

Affiliation notes

^I Deceased

^{II} Also at: Italian National Agency for New Technologies, Energy and Sustainable Economic Development (ENEA), Bologna, Italy

^{III} Also at: Dipartimento DET del Politecnico di Torino, Turin, Italy

^{IV} Also at: M.V. Lomonosov Moscow State University, D.V. Skobeltsyn Institute of Nuclear, Physics, Moscow, Russia

^V Also at: Department of Applied Physics, Aligarh Muslim University, Aligarh, India

^{VI} Also at: Institute of Theoretical Physics, University of Wrocław, Poland

^{VII} Also at: University of Kansas, Lawrence, Kansas, United States

Collaboration Institutes

¹ A.I. Alikhanyan National Science Laboratory (Yerevan Physics Institute) Foundation, Yerevan, Armenia

² AGH University of Science and Technology, Cracow, Poland

³ Bogolyubov Institute for Theoretical Physics, National Academy of Sciences of Ukraine, Kiev, Ukraine

⁴ Bose Institute, Department of Physics and Centre for Astroparticle Physics and Space Science (CAPSS), Kolkata, India

⁵ Budker Institute for Nuclear Physics, Novosibirsk, Russia

- ⁶ California Polytechnic State University, San Luis Obispo, California, United States
- ⁷ Central China Normal University, Wuhan, China
- ⁸ Centro de Aplicaciones Tecnológicas y Desarrollo Nuclear (CEADEN), Havana, Cuba
- ⁹ Centro de Investigación y de Estudios Avanzados (CINVESTAV), Mexico City and Mérida, Mexico
- ¹⁰ Chicago State University, Chicago, Illinois, United States
- ¹¹ China Institute of Atomic Energy, Beijing, China
- ¹² Chungbuk National University, Cheongju, Republic of Korea
- ¹³ Comenius University Bratislava, Faculty of Mathematics, Physics and Informatics, Bratislava, Slovakia
- ¹⁴ COMSATS University Islamabad, Islamabad, Pakistan
- ¹⁵ Creighton University, Omaha, Nebraska, United States
- ¹⁶ Department of Physics, Aligarh Muslim University, Aligarh, India
- ¹⁷ Department of Physics, Pusan National University, Pusan, Republic of Korea
- ¹⁸ Department of Physics, Sejong University, Seoul, Republic of Korea
- ¹⁹ Department of Physics, University of California, Berkeley, California, United States
- ²⁰ Department of Physics, University of Oslo, Oslo, Norway
- ²¹ Department of Physics and Technology, University of Bergen, Bergen, Norway
- ²² Dipartimento di Fisica dell'Università 'La Sapienza' and Sezione INFN, Rome, Italy
- ²³ Dipartimento di Fisica dell'Università and Sezione INFN, Cagliari, Italy
- ²⁴ Dipartimento di Fisica dell'Università and Sezione INFN, Trieste, Italy
- ²⁵ Dipartimento di Fisica dell'Università and Sezione INFN, Turin, Italy
- ²⁶ Dipartimento di Fisica e Astronomia dell'Università and Sezione INFN, Bologna, Italy
- ²⁷ Dipartimento di Fisica e Astronomia dell'Università and Sezione INFN, Catania, Italy
- ²⁸ Dipartimento di Fisica e Astronomia dell'Università and Sezione INFN, Padova, Italy
- ²⁹ Dipartimento di Fisica e Nucleare e Teorica, Università di Pavia, Pavia, Italy
- ³⁰ Dipartimento di Fisica 'E.R. Caianiello' dell'Università and Gruppo Collegato INFN, Salerno, Italy
- ³¹ Dipartimento DISAT del Politecnico and Sezione INFN, Turin, Italy
- ³² Dipartimento di Scienze e Innovazione Tecnologica dell'Università del Piemonte Orientale and INFN Sezione di Torino, Alessandria, Italy
- ³³ Dipartimento di Scienze MIFT, Università di Messina, Messina, Italy
- ³⁴ Dipartimento Interateneo di Fisica 'M. Merlin' and Sezione INFN, Bari, Italy
- ³⁵ European Organization for Nuclear Research (CERN), Geneva, Switzerland
- ³⁶ Faculty of Electrical Engineering, Mechanical Engineering and Naval Architecture, University of Split, Split, Croatia
- ³⁷ Faculty of Engineering and Science, Western Norway University of Applied Sciences, Bergen, Norway
- ³⁸ Faculty of Nuclear Sciences and Physical Engineering, Czech Technical University in Prague, Prague, Czech Republic
- ³⁹ Faculty of Science, P.J. Šafárik University, Košice, Slovakia
- ⁴⁰ Frankfurt Institute for Advanced Studies, Johann Wolfgang Goethe-Universität Frankfurt, Frankfurt, Germany
- ⁴¹ Fudan University, Shanghai, China
- ⁴² Gangneung-Wonju National University, Gangneung, Republic of Korea
- ⁴³ Gauhati University, Department of Physics, Guwahati, India
- ⁴⁴ Helmholtz-Institut für Strahlen- und Kernphysik, Rheinische Friedrich-Wilhelms-Universität Bonn, Bonn, Germany
- ⁴⁵ Helsinki Institute of Physics (HIP), Helsinki, Finland
- ⁴⁶ High Energy Physics Group, Universidad Autónoma de Puebla, Puebla, Mexico
- ⁴⁷ Hiroshima University, Hiroshima, Japan
- ⁴⁸ Hochschule Worms, Zentrum für Technologietransfer und Telekommunikation (ZTT), Worms, Germany
- ⁴⁹ Horia Hulubei National Institute of Physics and Nuclear Engineering, Bucharest, Romania
- ⁵⁰ Indian Institute of Technology Bombay (IIT), Mumbai, India
- ⁵¹ Indian Institute of Technology Indore, Indore, India
- ⁵² Indonesian Institute of Sciences, Jakarta, Indonesia
- ⁵³ INFN, Laboratori Nazionali di Frascati, Frascati, Italy
- ⁵⁴ INFN, Sezione di Bari, Bari, Italy
- ⁵⁵ INFN, Sezione di Bologna, Bologna, Italy
- ⁵⁶ INFN, Sezione di Cagliari, Cagliari, Italy
- ⁵⁷ INFN, Sezione di Catania, Catania, Italy

- 58 INFN, Sezione di Padova, Padova, Italy
59 INFN, Sezione di Pavia, Pavia, Italy
60 INFN, Sezione di Roma, Rome, Italy
61 INFN, Sezione di Torino, Turin, Italy
62 INFN, Sezione di Trieste, Trieste, Italy
63 Inha University, Incheon, Republic of Korea
64 Institute for Gravitational and Subatomic Physics (GRASP), Utrecht University/Nikhef, Utrecht, Netherlands
65 Institute for Nuclear Research, Academy of Sciences, Moscow, Russia
66 Institute of Experimental Physics, Slovak Academy of Sciences, Košice, Slovakia
67 Institute of Physics, Homi Bhabha National Institute, Bhubaneswar, India
68 Institute of Physics of the Czech Academy of Sciences, Prague, Czech Republic
69 Institute of Space Science (ISS), Bucharest, Romania
70 Institut für Kernphysik, Johann Wolfgang Goethe-Universität Frankfurt, Frankfurt, Germany
71 Instituto de Ciencias Nucleares, Universidad Nacional Autónoma de México, Mexico City, Mexico
72 Instituto de Física, Universidade Federal do Rio Grande do Sul (UFRGS), Porto Alegre, Brazil
73 Instituto de Física, Universidad Nacional Autónoma de México, Mexico City, Mexico
74 iThemba LABS, National Research Foundation, Somerset West, South Africa
75 Jeonbuk National University, Jeonju, Republic of Korea
76 Johann-Wolfgang-Goethe Universität Frankfurt Institut für Informatik, Fachbereich Informatik und Mathematik, Frankfurt, Germany
77 Joint Institute for Nuclear Research (JINR), Dubna, Russia
78 Korea Institute of Science and Technology Information, Daejeon, Republic of Korea
79 KTO Karatay University, Konya, Turkey
80 Laboratoire de Physique des 2 Infinis, Irène Joliot-Curie, Orsay, France
81 Laboratoire de Physique Subatomique et de Cosmologie, Université Grenoble-Alpes, CNRS-IN2P3, Grenoble, France
82 Lawrence Berkeley National Laboratory, Berkeley, California, United States
83 Lund University Department of Physics, Division of Particle Physics, Lund, Sweden
84 Moscow Institute for Physics and Technology, Moscow, Russia
85 Nagasaki Institute of Applied Science, Nagasaki, Japan
86 Nara Women's University (NWU), Nara, Japan
87 National and Kapodistrian University of Athens, School of Science, Department of Physics, Athens, Greece
88 National Centre for Nuclear Research, Warsaw, Poland
89 National Institute of Science Education and Research, Homi Bhabha National Institute, Jatni, India
90 National Nuclear Research Center, Baku, Azerbaijan
91 National Research Centre Kurchatov Institute, Moscow, Russia
92 Niels Bohr Institute, University of Copenhagen, Copenhagen, Denmark
93 Nikhef, National institute for subatomic physics, Amsterdam, Netherlands
94 NRC Kurchatov Institute IHEP, Protvino, Russia
95 NRC «Kurchatov» Institute - ITEP, Moscow, Russia
96 NRNU Moscow Engineering Physics Institute, Moscow, Russia
97 Nuclear Physics Group, STFC Daresbury Laboratory, Daresbury, United Kingdom
98 Nuclear Physics Institute of the Czech Academy of Sciences, Řež u Prahy, Czech Republic
99 Oak Ridge National Laboratory, Oak Ridge, Tennessee, United States
100 Ohio State University, Columbus, Ohio, United States
101 Petersburg Nuclear Physics Institute, Gatchina, Russia
102 Physics department, Faculty of science, University of Zagreb, Zagreb, Croatia
103 Physics Department, Panjab University, Chandigarh, India
104 Physics Department, University of Jammu, Jammu, India
105 Physics Department, University of Rajasthan, Jaipur, India
106 Physikalisches Institut, Eberhard-Karls-Universität Tübingen, Tübingen, Germany
107 Physikalisches Institut, Ruprecht-Karls-Universität Heidelberg, Heidelberg, Germany
108 Physik Department, Technische Universität München, Munich, Germany
109 Politecnico di Bari and Sezione INFN, Bari, Italy
110 Research Division and ExtreMe Matter Institute EMMI, GSI Helmholtzzentrum für Schwerionenforschung GmbH, Darmstadt, Germany

- 111 Russian Federal Nuclear Center (VNIIEF), Sarov, Russia
- 112 Saha Institute of Nuclear Physics, Homi Bhabha National Institute, Kolkata, India
- 113 School of Physics and Astronomy, University of Birmingham, Birmingham, United Kingdom
- 114 Sección Física, Departamento de Ciencias, Pontificia Universidad Católica del Perú, Lima, Peru
- 115 St. Petersburg State University, St. Petersburg, Russia
- 116 Stefan Meyer Institut für Subatomare Physik (SMI), Vienna, Austria
- 117 SUBATECH, IMT Atlantique, Université de Nantes, CNRS-IN2P3, Nantes, France
- 118 Suranaree University of Technology, Nakhon Ratchasima, Thailand
- 119 Technical University of Košice, Košice, Slovakia
- 120 The Henryk Niewodniczanski Institute of Nuclear Physics, Polish Academy of Sciences, Cracow, Poland
- 121 The University of Texas at Austin, Austin, Texas, United States
- 122 Universidad Autónoma de Sinaloa, Culiacán, Mexico
- 123 Universidade de São Paulo (USP), São Paulo, Brazil
- 124 Universidade Estadual de Campinas (UNICAMP), Campinas, Brazil
- 125 Universidade Federal do ABC, Santo Andre, Brazil
- 126 University of Cape Town, Cape Town, South Africa
- 127 University of Houston, Houston, Texas, United States
- 128 University of Jyväskylä, Jyväskylä, Finland
- 129 University of Kansas, Lawrence, Kansas, United States
- 130 University of Liverpool, Liverpool, United Kingdom
- 131 University of Science and Technology of China, Hefei, China
- 132 University of South-Eastern Norway, Tonsberg, Norway
- 133 University of Tennessee, Knoxville, Tennessee, United States
- 134 University of the Witwatersrand, Johannesburg, South Africa
- 135 University of Tokyo, Tokyo, Japan
- 136 University of Tsukuba, Tsukuba, Japan
- 137 Université Clermont Auvergne, CNRS/IN2P3, LPC, Clermont-Ferrand, France
- 138 Université de Lyon, CNRS/IN2P3, Institut de Physique des 2 Infinis de Lyon, Lyon, France
- 139 Université de Strasbourg, CNRS, IPHC UMR 7178, F-67000 Strasbourg, France, Strasbourg, France
- 140 Université Paris-Saclay Centre d'Etudes de Saclay (CEA), IRFU, Département de Physique Nucléaire (DPHN), Saclay, France
- 141 Università degli Studi di Foggia, Foggia, Italy
- 142 Università di Brescia, Brescia, Italy
- 143 Variable Energy Cyclotron Centre, Homi Bhabha National Institute, Kolkata, India
- 144 Warsaw University of Technology, Warsaw, Poland
- 145 Wayne State University, Detroit, Michigan, United States
- 146 Westfälische Wilhelms-Universität Münster, Institut für Kernphysik, Münster, Germany
- 147 Wigner Research Centre for Physics, Budapest, Hungary
- 148 Yale University, New Haven, Connecticut, United States
- 149 Yonsei University, Seoul, Republic of Korea